Structure of Dense Polymer Layers between End-Grafting and End-Adsorbing Walls

E. B. Zhulina† and T. Pakula*

Max-Planck-Institut für Polymerforschung, Postfach 3148, W-6500 Mainz, FRG

Received May 20, 1991; Revised Manuscript Received September 26, 1991

ABSTRACT: The structure of a polymer melt layer confined between two parallel walls in which the chains are grafted at one of their ends to a wall and interact with their free ends with the opposite wall is considered. The theoretical solution based on the self-consistent-field theory is presented and compared with results of the computer simulation performed by means of the cooperative rearrangements method. Both the theory and the simulation show that the structure of the layer can be regarded as consisting of end-rich and end-poor zones adjacent to end-grafting and end-adsorbing walls, respectively. The relative extent of the zones can be influenced by the adsorption energy.

Introduction

Theoretical investigation of grafted layers, i.e., layers of polymer chains grafted at one end onto an impermeable surface, is interesting because of numerous applications. The analysis of the equilibrium behavior of such layers provides important information related to the structure of block copolymers at the interface, to the structure in micellar solutions, and to superstructure formation in block copolymer systems under the conditions of microphase separation. At present, such grafted layers are the subject of intensive investigation in both theory and experiment (see, for example, ref 1).

In this paper we consider a special case of dense planar grafted layers consisting of polymer chains grafted at one wall (A) and interacting with the opposite wall (B) by functionalized end groups (Figure 1). This investigation is within a framework of a broader project dealing with a computer simulation of thin polymer layers.[2,3] Here, however, we present a theoretical solution of the problem as well. We consider a layer formed by flexible chains consisting of $N \gg 1$ units at grafting density σ. For the sake of generality we assume that chain units are asymmetrical with a cross-sectional area s_0 and length a. A stiffness parameter p of chains is considered relating their average end-to-end distance $\langle R^2 \rangle$ with the chain length, $\langle R^2 \rangle = pa^2N$. We assume that free ends of grafted chains can adsorb at the outer boundary of the layer, thus giving the energy gain ϵ per adsorbed chain.

Such a grafted layer with adsorbing free ends was considered recently by Johner and Joanny[4] for the case when the layer is immersed in a good solvent. They used the self-consistent-field (SCF) approach developed earlier for grafted chains with inert free ends.[5-7] One of the main results of this paper was the prediction of the so-called "dead" zone, i.e., a zone without free ends located at the periphery of the layer. The appearance of the dead zone is a result of the constraints imposed on the positions of free chain ends adsorbed at the outer boundary of the layer. Hence, one can expect that a similar zone will appear in a dense layer of grafted chains with end-adsorbing groups. The aim of this paper is to prove the above expectations by computer simulation and to compare them with relevant theoretical predictions. In order to make such a comparison possible, we first extend the approach of ref 4 to the case of dense layers (without solvent) and then compare our theoretical results with the results of the computer simulation.

† On leave from the Institute of Macromolecular Compounds of the Academy of Sciences of the USSR, 199004 Leningrad, USSR.

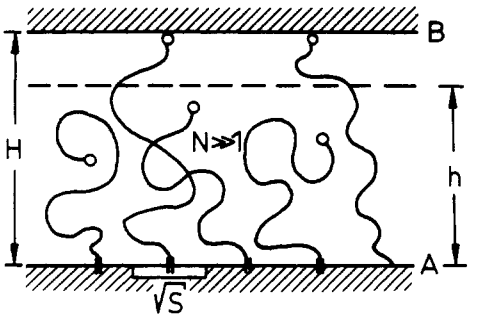

Figure 1. Schematic illustration of the model of a planar layer of thickness H with chains grafted at one wall (A) and adsorbing at the other wall (B) by end-functionalized groups. Nonadsorbed chains form a sublayer of thickness h.

Theory

At given values of N and $\sigma = s_0/s$ the equilibrium structure of a dense layer is determined by the fraction q of adsorbed chains. Under the condition of considerable stretching of grafted chains with respect to their Gaussian dimension, the dead zone forms at $q \neq 0$. The free ends of nonadsorbed chains avoid the periphery part of the layer near the outer boundary, where only units of adsorbed chains are located. In this zone adsorbed chains are stretched uniformly and homogeneously. The units of nonadsorbed chains and the tie part of adsorbed chains fill the sublayers of thickness h adjacent to the grafting surface. In this sublayer of thickness h, chains experience SCF potential and are stretched inhomogeneously, the distribution function $g(x)$ describing the partitioning of their free ends. At given fraction $q < 1$ of adsorbed chains, the free energy of the layer per chain is given by the SCF functional

$$\Delta F = \frac{3}{2a^2p}[(1-q)\int_0^h g(x')\,dx'\int_0^{x'} E_n(x,x')\,dx + q\int_0^h E_a(x)\,dx] + \frac{3}{2a^2p}qE_a(h)\,(H-h) - q\epsilon \quad (1)$$

where $E_n = (dx/dn)_n$ and $E_a = (dx/dn)_a$ are the functions of local stretching of nonadsorbed and adsorbed chains, respectively. (Here and below, all energetic quantities are in kT units.) The first two terms in (1) describe the inhomogeneous stretching of nonadsorbed chains and the tie parts of adsorbed chains in the sublayer of thickness h, the third term describes the homogeneous stretching of

0024-9297/92/2225-0754$03.00/0

adsorbed chains in the dead zone of thickness $(H-h)$, and the last term is the adsorption energy gain.

Minimization of (1) with due account of the chain-length conservation

$$\int_0^{x'} \frac{dx}{E_n(x,x')} = \int_0^H \frac{dx}{E_a(x)} = N \tag{2}$$

and of the dense layer packing

$$\frac{as_0}{s}\left[(1-q)\int_0^x \frac{g(x')\,dx'}{E_n(x,x')} + q\frac{1}{E_a(x)}\right] = 1 \tag{3}$$

provides structural characteristics of the layer (see ref 5 for technical details):

(a) the functions characterizing the local stretching of chains

$$E_n(x,x') = \frac{\pi}{2N}(y^2-x^2)^{1/2} \qquad x \le y \le h \tag{4}$$

$$E_a(x) = \begin{cases} \dfrac{\pi}{2N}\left[\dfrac{h^2}{\cos^2\left[\frac{\pi}{2}\tau\right]} - x^2\right]^{1/2} & x \le h \\ \dfrac{\pi}{2N}htg\left[\dfrac{\pi}{2}\tau\right] & h < x < H \end{cases} \tag{5}$$

where τ is the fraction of units of the adsorbed chain in the dead zone related to the fraction q of adsorbed chains as

$$q = \frac{\pi}{2}(1-q\tau)tg\left[\frac{\pi}{2}\tau\right] \tag{6}$$

(b) the concentration profiles of units of nonadsorbed and adsorbed chains

$$\varphi_n(x) = 1 - q\frac{2}{\pi}\frac{1}{\left[\dfrac{(1-q\tau)^2}{\cos^2\left(\frac{\pi}{2}\tau\right)} - \dfrac{x^2}{H^2}\right]^{1/2}} \tag{7}$$

$$\varphi_a(x) = 1 - \varphi_n(x)$$

(c) the distribution function of nonadsorbed ends, $\bar{g}(x') = g(x')\,(1-q)$

$$\bar{g}(x') = \frac{x'}{H^2}\frac{\left[(1-q\tau)^2 - \dfrac{(x')^2}{H^2}\right]^{1/2}}{\dfrac{(1-q\tau)}{\cos^2\left(\frac{\pi}{2}\tau\right)} - \dfrac{(x')^2}{H^2}} \tag{8}$$

and the total distribution function of nongrafted ends

$$g_t(x') = (1-q)g(x') + q\delta(H-x') \tag{9}$$

where $\delta(t)$ is the delta function.

(d) the distribution function of centers of inertia of nonadsorbed chains

$$\bar{g}_c(x_c) = \frac{\pi}{2}g\left(\frac{\pi}{2}x_c\right) \tag{10}$$

and that of all chains

$$g_c(x_c) = \bar{g}_c(x_c) + q\delta(x - x_c^a) \tag{11}$$

where

$$x_c^a = H\left\{\frac{2}{\pi}(1-q\tau)\left[\frac{1-\sin(\pi\tau/2)}{\cos(\pi\tau/2)}\right] + \frac{\tau}{2}(2-q\tau)\right\} \tag{12}$$

is the position of the center of inertia of adsorbed chains.

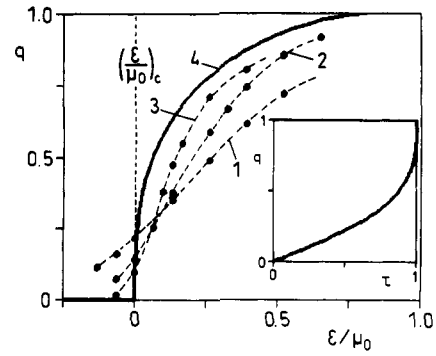

Figure 2. Fraction q of adsorbed chains as a function of the interaction energy between the functionalized ends and the adsorbing wall. The solid line (curve 4) represents the theoretical dependence as described by (11), and the filled points represent the computer-simulated results for systems with various chain lengths: (curve 1) $N = 40$, (curve 2) $N = 80$, (curve 3) $N = 160$. The inset shows the dependence between q and τ (the thickness of the "dead" zone) according to (6).

Substitution of (4), (5), and (8) into the functional (1) gives the free energy of the layer with a fixed fraction q of adsorbed ends

$$\Delta F = \frac{Ns_0^2}{s^2p}\left[\frac{\pi^2}{8}(1-q\tau)^3 + \frac{3}{2}q^2\right] - q\epsilon \tag{13}$$

(Note that, for the case of inert ends, $\epsilon = 0$ and $q = 0$, the relationship (13) reduces to the known result[5] $\Delta F = \Delta F_0 = (\pi^2/8)(Ns_0^2/s^2p)$.)

Finally, the equilibrium fraction q of adsorbed chains is obtained from the condition $\partial\Delta F/\partial q = 0$ to give

$$\frac{4}{\pi^2}q - \tau(1-q\tau)^2 = \epsilon/3\Delta F_0 = \epsilon/\mu_0 \tag{14}$$

where $\mu_0 = \Delta F_0 - s(\partial\Delta F_0/\partial s)$ is the chemical potential of grafted chains with inert ends ($\epsilon = 0$) in the layer. Equations 6 and 14 determine the adsorption isotherm $q = q(\epsilon)$ for the dense grafted layer with given values of $N \gg 1$, σ, and ϵ (Figure 2). The concentration profiles of chain units, $\varphi_n(x)$, and of the free ends $\bar{g}(x')$ are presented in Figures 3a and 4a.

Results of the Simulation

The simulation has been carried out using the algorithm based on cooperative rearrangements in a system of chains on the face-centered cubic (fcc) lattice with all lattice sites occupied. The algorithm of the simulation has been described in detail in several previous papers.[8,9] Layers consisting of linear chains confined between two parallel walls have been considered. For this type of lattice, each chain unit related to the bond length $l = a\sqrt{2}$ occupies the volume $2a^3$. The walls of the layer are chosen in such a way that in the direction of the layer thickness the cross-sectional area of a chain is $s_0 = 2a^2$ and the length of the chain unit coincides with the lattice constant a. As has been shown in earlier simulations,[2] the mean-squared end-to-end distance $\langle R^2\rangle$ for nongrafted chains in a melt on such a lattice is described with good accuracy by the relationship[10]

$$\langle R^2\rangle = Nl^2\frac{1+(z_c-1)^{-1}}{1-(z_c-1)^{-1}} = 2.4Na^2 \tag{15}$$

where $z_c = 12$ is the coordination number of the fcc lattice. Hence, the value of the stiffness parameter $p = 2.4$. The chains of various lengths ($N = 40, 80$, and 160) were grafted at one wall (A) with density $\sigma = 0.5$ ensuring a relatively

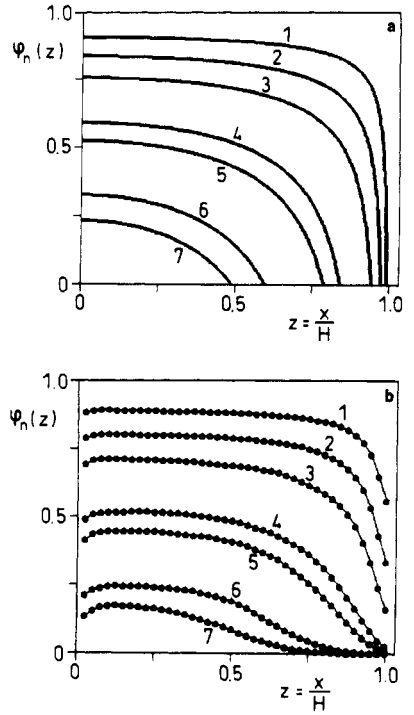

Figure 3. Concentration profiles of units of nonadsorbed chains (a) as predicted by the theory and (b) as determined for the simulated systems with various interaction energies between end-functionalized groups and the adsorbing wall. The theoretical dependencies are plotted for the same fractions of adsorbed chains as observed in the simulation: (1) 0.145, (2) 0.259, (3) 0.372, (4) 0.593, (5) 0.671, (6) 0.856, (7) 0.918.

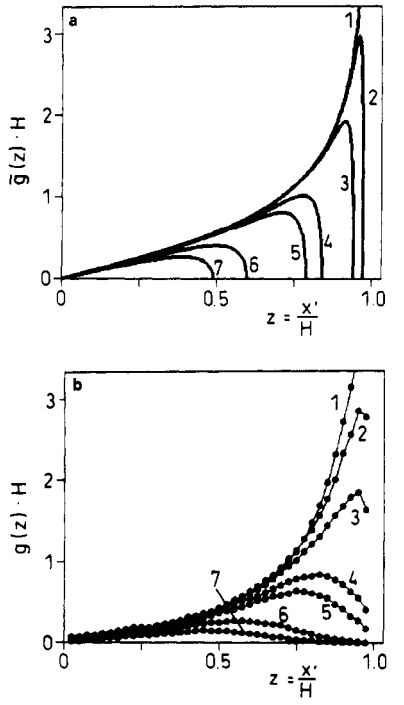

Figure 4. Distributions of nonadsorbed ends (a) as predicted by the theory and (b) as observed in the simulated systems. The theoretical curves are plotted for the q values determined for the simulated systems; the same as in Figure 3.

high stretching of chains with respect to their relaxed dimensions in an isotropic melt. The grafted ends were left mobile at the grafting wall. The nongrafted ends of chains have been regarded as being functionalized and interacting with the opposite wall (B), separated from the grafting wall by $H = \sigma Na$ (given by the condition of high density, $\rho = 1$). The interaction has been introduced by assuming that for the functionalized ends the states at the adsorbing wall and away from it can differ in potential energy by $\Delta\epsilon$. Consequently for an attractive interaction ($\Delta\epsilon > 0$), moves involving a separation of the functionalized chain end from the wall have been performed with the probability $w_+ = w_0 \exp(-\Delta\epsilon)$, where w_0 is the probability of leaving the wall in the absence of the specific interaction. In the case of repulsive interaction ($\Delta\epsilon < 0$), moves toward the wall were performed with the probability $w_- = w_0 \exp(\Delta\epsilon)$. The attractive interaction led to the adsorption of the functionalized ends at the wall depending on $\Delta\epsilon$. Densities of chain ends adsorbed at the wall in systems equilibrated under the above conditions with various $\Delta\epsilon$ and N values are shown in Figure 2 (full circles) in comparison with the theoretical curve (solid line). As is seen from Figure 2, for all N values an increase of the adsorption energy $\epsilon = \Delta\epsilon$ in the simulated system leads to a corresponding increase of the number of chain ends adsorbed at the wall. But the theoretical dependence is not reproduced exactly by the simulated results. The deviations decrease, however, with an increase in the length of the chains in the simulated systems.

Qualitatively, such behavior resembles that observed for polymers adsorbing onto a planar surface from a dilute solution. It was shown[11-13] that in the latter case the adsorption of an isolated infinitely long polymer chain on a planar surface occurs as a phase transition. If for such an adsorbing chain each contact of the chain with the surface leads to energy gain ϵ per chain unit, the fraction Q of adsorbed polymer units depends on ϵ in a critical manner: i.e., $Q = 0$ below a certain critical value of adsorption energy ϵ_c, $\epsilon < \epsilon_c$, while at $\epsilon > \epsilon_c$ Q increases with ϵ approaching unity at $\epsilon \to \infty$. Characteristics of this transition, i.e., values of the critical energy ϵ_c, order of the transition (determined as the value of exponent r in the expansion of the free energy of the system in the vicinity of the critical point, $\delta F \sim -(\epsilon - \epsilon_c)^r$), etc., depend on the details of the chain model considered (thermodynamic stiffness, solvent quality, etc.). For example, for the simplest case of flexible Gaussian chains ($N \to \infty$), adsorption on a planar surface occurs as a transition of the second order ($r = 2$) and the value of the critical energy ϵ_c is on the order of $10^{-1}kT$.[13] It was demonstrated that, for this kind of transition, for finite N values, the adsorption isotherms are smoothed considerably; i.e., $Q > 0$ at $\epsilon < \epsilon_c$.[14]

As seen in Figure 2, similar regularities take place in our case of end-adsorbing grafted chains. This suggests that bridging of a dense layer by chains grafted at one wall can perhaps be considered as a phase transition as well. For infinitely long chains where the SCF theory becomes asymptotically rigorous, an analysis of theoretical curves $q = q(\epsilon/\mu_0)$ can provide relevant characteristics of the adsorption process in a dense layer. Taking into account that for $N \to \infty$ the fraction of adsorbed ends $q = 0$ at $\epsilon/\mu_0 = 0$ and consequently $q = 0$ at all values $\epsilon/\mu_0 < 0$, one can regard the bridging of the layer by such chains as occurring with the critical point $(\epsilon/\mu_0)_c = 0$. An expansion of (14) for small ϵ/μ_0 values, $\epsilon/\mu_0 \ll 1$, allows a determination of the order of this transition. Taking into account (6), we obtain

$$q \simeq \left(\frac{3\pi^4}{64}\frac{\epsilon}{\mu_0}\right)^{1/3} \tag{16}$$

and, correspondingly, at $\epsilon/\mu_0 > 0$ the equilibrium free

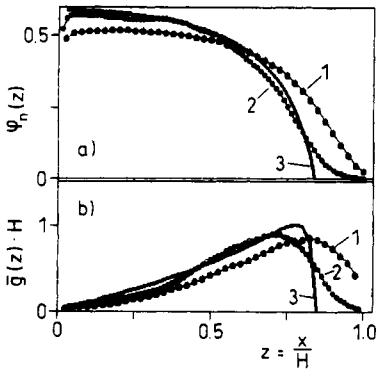

Figure 5. Illustration of the effect of the chain length on (a) the concentration profiles of units of nonadsorbed chains and (b) the distributions of nonadsorbed ends: (1) $N = 80$, (2) $N = 160$, (3) theoretical dependencies $N \to \infty$; in all cases ϵ/μ_0 = constant.

energy of the system scales as

$$\delta F = \frac{\Delta F_{eq} - \Delta F_0}{\Delta F_0} \simeq -\left(\frac{\epsilon}{\mu_0}\right)^{4/3} \qquad (17)$$

Hence, for the infinitely long grafted chains adsorption of free ends at the outer boundary of a dense planar layer occurs as a phase transition of the order $r = {}^4/_3$. For finite N values used in the simulation, the adsorption curves $q = q(\epsilon/\mu_0)$ are considerably smoothed with respect to the limiting case $N \to \infty$ but increasing N leads to better agreement with the theoretical dependence (curve 4 in Figure 2).

Let us compare now the structural characteristics of the layers. For chains which are not adsorbed the distributions of segment densities and the distributions of chain-end concentrations have been determined. The results are shown in Figures 3b and 4b. Equivalent theoretical dependencies calculated for the same q values as in the simulated systems are shown in Figures 3a and 4a by thick solid lines. As is seen from Figure 3b, the density profiles of nonadsorbed chains became more steep with increasing q and, at high values of q, nonadsorbed chains do not reach the periphery part of the layer. A comparison of theoretical predictions with the results of the simulation shows that simulated profiles tend to zero much more smoothly than the theoretical ones. The origin of these discrepancies is the fluctuations which are totally ignored within the SCF approach used. An increase in the molecular weight of grafted chains N leads to better agreement between the simulated results and the theoretical curves as illustrated in Figure 5 by a comparison of the theoretical distributions ($N \to \infty$) with dependencies simulated for two different chain lengths.

Similar conclusions can be drawn from a comparison of the theoretical and simulated distributions of nonadsorbed ends (Figure 4). Here, the maxima of the concentration of chain ends shift away from the adsorbing wall with increasing $\Delta\epsilon$ in the same way as the theoretical distributions show. However, in contrast to the theoretical distributions, the chain ends do not disappear completely from the zone close to the adsorbing wall and therefore for finite N values it should rather be called an "end-poor" zone. This end-poor zone transforms into a dead zone (Figure 5b) with increasing chain stretching, i.e., increasing N and/or σ.

Figure 6a shows the distributions of centers of mass in simulated systems. With increasing adsorption energy the main maximum of the distribution shifts toward the center of the layer indicating an increasing fraction of chains bridging the walls. At higher adsorption energies

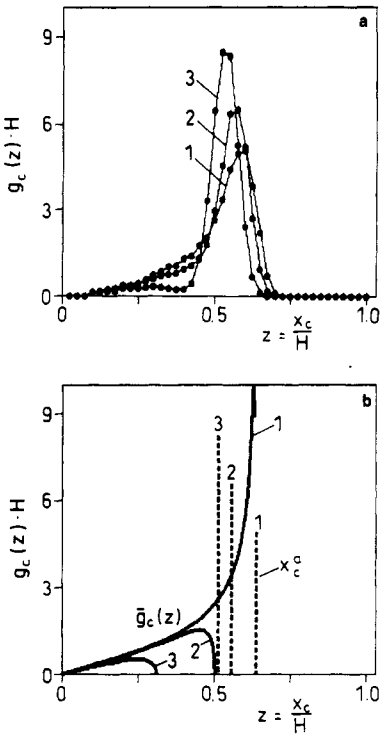

Figure 6. (a) Center-of-mass distributions of grafted chains in simulated dense layers with various adsorption energies between functionalized ends and the adsorbing wall. Curves 1–3 correspond to systems represented in Figure 3 and 4 by curves 1, 5, and 7, respectively. (b) Center-of-mass distributions as described by (11) (the solid lines represent the fraction of nonadsorbed chains (eq 10), and the broken lines show the positions of the center of mass for adsorbed chains (eq 12). Curves 1–3 are calculated for q values corresponding to cases 1–3 in Figure 6a.

the centers of mass of nonadsorbed chains show another maximum at smaller distances from the grafting wall. This is in qualitative agreement with dependencies (10) and (12) given by the theory as illustrated graphically in Figure 6b for q values the same as determined for the simulated systems considered in Figure 6a.

Conclusions

The results of computer simulation have shown that, in layers with chains grafted at one wall and interacting by their functionalized free ends with the other wall, a peculiar structure is formed consisting of a free end-rich sublayer adjacent to the grafting wall and a free end-poor layer adjacent to the adsorbing wall. The proportions of the thickness of these sublayers can be influenced by the interaction energy between the functionalized ends and the adsorbing wall. It influences the number of chains bridging the outer walls of the layer and leads to redistribution of the entropic elasticity of chains. An increase of the molecular weight of grafted chains at fixed values of adsorption energy and grafting density disfavors bridging of walls by adsorbed chains. As also pointed out in ref 4, the bridging is governed by the ratio ϵ/μ_0, where $\mu_0 \approx N(s/s_0)^{-2}$ is the chemical potential of a grafted dense layer. Consequently, in high molecular weight grafted layers noticeable bridging can only be expected for high values of adsorption energy $\epsilon \sim N$. In the limit $N \to \infty$ the bridging process in a dense layer occurs as a phase transition of the order $r = {}^4/_3$ with the critical value of the reduced adsorption energy $(\epsilon/\mu_0)_c = 0$.

A similar process in a swollen layer (i.e., layer immersed in a good solvent) occurs more smoothly. In this case the fraction q_{sw} of adsorbed ends scales linearly with ϵ, $q_{sw} \sim$

(ϵ/μ_0^{sw}), where $\mu_0^{sw} \simeq N(s/s_0)^{-2/3}$ is the chemical potential of a grafted chain in a swollen brush.[4] A simple estimation shows that at the same values of adsorption energy ϵ/N = constant $\ll 1$ the ratio $q/q_{sw} \simeq (\epsilon/N)^{-2/3} \gg 1$ and, thus, swelling of a brush diminishes the ability of bridging. Physical reasons for that are evident: in a swollen layer chains are more stretched than in a dense layer, $\mu_0^{sw} \geq \mu_0$; hence, more energy is necessary to compensate the loss of entropy of a chain with an adsorbed free end. In the limit $N \to \infty$ swelling effects change the character of the bridging process, transforming it into a phase transition of higher order, $r = 2$.

Generally, we can conclude that a good agreement between the simulated and theoretical results has been found. Both results indicated that chains in dense systems between end-grafting and end-adsorbing walls form complex, heterogeneous structures strongly dependent on the adsorption energy of the functionalized ends. It should be emphasized that such effects can appear in a number of systems, like, for example, in triblock copolymers with lamellar structures, in lamellarly crystallizing polymers, or at surfaces coated with grafted polymers. An understanding of these effects can be used as a guide to the modification of the structure and properties (mechanical or optical) of such systems.

Acknowledgment. E.B.Z. acknowledges the hospitality of Prof. G. Wegner in the Max-Planck-Institut für Polymerforschung and the financial support of the A. v. Humboldt Foundation.

References and Notes

(1) Halperin, A.; Tirrell, M.; Lodge, T. P. Tethered Chains in Polymer Microstructures. *Adv. Polym. Sci.* **1991**, *100*, in press.
(2) Pakula, T. *J. Chem. Phys.* **1991**, *95*, 4685.
(3) Pakula, T.; Zhulina, E. B. *J. Chem. Phys.* **1991**, *95*, 4691.
(4) Johner, A.; Joanny, J. F. *Europhys. Lett.* **1991**, *15*, 265.
(5) Semenov, A. N. *Sov. Phys. JETP* **1985**, *61*, 733.
(6) Skvortsov, A. M.; Pavlushkov, I. V.; Gorbunov, A. A.; Zhulina, E. B.; Borisov, O. V.; Promitsyn, V. A. *Polym. Sci. USSR* **1988**, *30*, 1706.
(7) Milner, S.; Witten, T.; Cates, M. *Europhys. Lett.* **1988**, *5*, 413; *Macromolecules* **1988**, *21*, 2610.
(8) Pakula, T. *Macromolecules* **1987**, *20*, 679.
(9) Reiter, J.; Edling, T.; Pakula, T. *J. Chem. Phys.* **1990**, *93*, 837.
(10) Yamakawa, H. *Modern Theory of Polymer Solutions*; Harper and Row: New York, 1971.
(11) Di Marzio, E. A.; McCrakin, F. L. *J. Chem. Phys.* **1965**, *43*, 539.
(12) Rubin, R. J. *J. Chem. Phys.* **1965**, *43*, 2392.
(13) Birstein, T. M. *Macromolecules* **1979**, *12*, 715.
(14) Skvortsov, A. M.; Birstein, T. M., Zhulina, E. B. *Polym. Sci. USSR* **1976**, *18*, 2276.